ACTA ONCOLOGICA, 2017
VOL. 56, NO. 11, 1604–1609
https://doi.org/10.1080/0284186X.2017.1373848

Taylor & Francis
Taylor & Francis Group

ORIGINAL ARTICLE

Difference in target definition using three different methods to include respiratory motion in radiotherapy of lung cancer

Ditte Sloth Møller[a], Marianne Marquard Knap[b], Tine Bisballe Nyeng[a], Azza Ahmed Khalil[b], Marianne Ingerslev Holt[b], Maria Kandi[b] and Lone Hoffmann[a]

[a]Department of Medical Physics, Aarhus University Hospital, Aarhus C, Denmark; [b]Department of Oncology, Aarhus University Hospital, Aarhus C, Denmark

ABSTRACT

Introduction: Minimizing the planning target volume (PTV) while ensuring sufficient target coverage during the entire respiratory cycle is essential for free-breathing radiotherapy of lung cancer. Different methods are used to incorporate the respiratory motion into the PTV.

Material and methods: Fifteen patients were analyzed. Respiration can be included in the target delineation process creating a respiratory GTV, denoted iGTV. Alternatively, the respiratory amplitude (A) can be measured based on the 4D-CT and A can be incorporated in the margin expansion. The GTV expanded by A yielded GTV + resp, which was compared to iGTV in terms of overlap. Three methods for PTV generation were compared. PTV_{del} (delineated iGTV expanded to CTV plus PTV margin), PTV_{σ} (GTV expanded to CTV and A was included as a random uncertainty in the CTV to PTV margin) and $PTV_{\sum}$ (GTV expanded to CTV, succeeded by CTV linear expansion by A to CTV + resp, which was finally expanded to $PTV_{\sum}$).

Results: Deformation of tumor and lymph nodes during respiration resulted in volume changes between the respiratory phases. The overlap between iGTV and GTV + resp showed that on average 7% of iGTV was outside the GTV + resp implying that GTV + resp did not capture the tumor during the full deformable respiration cycle. A comparison of the PTV volumes showed that PTV_{σ} was smallest and PTV_{Σ} largest for all patients. PTV_{σ} was in mean 14% (31 cm^3) smaller than PTV_{del}, while PTV_{del} was 7% (20 cm^3) smaller than PTV_{Σ}.

Conclusions: PTV_{σ} yields the smallest volumes but does not ensure coverage of tumor during the full respiratory motion due to tumor deformation. Incorporating the respiratory motion in the delineation (PTV_{del}) takes into account the entire respiratory cycle including deformation, but at the cost, however, of larger treatment volumes. PTV_{Σ} should not be used, since it incorporates the disadvantages of both PTV_{del} and PTV_{σ}.

ARTICLE HISTORY
Received 9 May 2017
Accepted 25 August 2017

Introduction

Radiotherapy of lung cancer is challenging due to a high risk of toxicity when delivering curative doses [1–3]. Keeping the treatment volumes as small as possible while treating the whole target volume is therefore essential. Margins in radiotherapy take into account the different uncertainties associated with planning and delivering radiotherapy, ensuring sufficient target coverage [4–5]. Population-based uncertainties are used for delivery uncertainties and inter- and intrafractional uncertainties [6–9]. On the other hand, the respiratory motion can be measured pretreatment for each patient and should therefore be taken into account patient specifically. Different methods to obtain patient-specific margins are available. The respiration can be incorporated into the delineation of the gross tumor volume (GTV) [10–12] or the center of mass (CM) peak-to-peak amplitude (A) can be measured and introduced as a random uncertainty in the margin calculation [4,13–15]. The two concepts are conceptually different, and in this study, we compare these two concepts in terms of the size of treatment volumes generated and in terms of their ability to take into account the respiration cycle including target deformation during respiration.

Material and methods

Patient selection

Fifteen consecutive patients with lung cancer treated with definitive chemo-radiotherapy were selected for the study. The study group consisted of four SCLC patients, 10 NSCLC patients and one patient with a NSCLC recurrence. Staging was IIIa (7pts), IIIb (4 pts), IIa (1 pt), IIb (2pts) and Ia (1pt). The median age was 69 years [53–77 years]. Eleven females and four males were included. Stage, histology, performance status and tumor and lymph node location was displayed for each patient in Table 1.

CONTACT Ditte Sloth Møller dittmoel@rm.dk Aarhus University Hospital, Department of Medical Physics, Noerrebrogade 44, building 5J, 2. Floor, 8000 Aarhus C, Denmark

Table 1. Characteristic and respiratory motion for each patient.

						Volume [cm^3]		Resp. A, GTV-T [mm]			Resp. A, GTV-N [mm]		
Patient number	NSCLC /SCLC	Stage	GTV-T Location*	GTV-N Station £	PS	GTV-T	GTV-N	LR	AP	SI	LR	AP	SI
1	SCLC	IIIa	LU	5	1	19	1	3	2	2	2	1	1
2	SCLC	IIIb	RU	3A; 4R + 10R	1	10	37	2	3	3	3	3	2
3	NCSLC	IIb	RU + M	–	1	67	–	2	2	4	–	–	–
4	NSCLC	IIIa	LU	4L,5 + 10L	0	4	6	3	5	1	3	1	3
5	NSCLC	IIIb#	RU + M+L	–	1	361	–	6	3	5	–	–	–
6	SCLC	Ia	RU	–	2	22	–	1	1	2	–	–	–
7	NSCLC	IIIb	RU	4R	0	9	29	1	2	2	1	3	5
8	NSCLC	IIb	RL	3A, 4R, 7, 11R	2	64	19	1	2	11	3	5	7
9	NSCLC	IIa	RL	–	0	46	–	2	3	5	–	–	–
10	NSCLC rec	IIIa	–	7,10L	1	–	4	–	–	–	5	1	7
11	SCLC	IIIa	LU + L	4L,7	2	17	11	2	2	4	2	1	3
12	NSCLC	IIIa	RU	4R	1	10	18	2	6	11	2	2	6
13	NSCLC	IIIa	LU	4L;5	0	14	5	5	2	5	1	4	9
14	NSCLC	IIIa	RL	2R + 4R + 7 + 10R + 11R	2	15	126	1	5	16	4	2	9
15	NSCLC	IIIb	RU	4R,7	0	4	8	2	1	1	1	1	3

#Undistinguishable tumor and lymph node conglomerate.
*L: left; L: lower lobe; M: middle lobe; R: right; U: upper lobe. £According to [27]. Conglomerates of nodes are marked by a plus.

Target definition

A combined phase-sorted 4D-CT with 10 phases and 3D FDG-PET scan were acquired on a Phillips PET-CT scanner for all patients for radiotherapy planning. The 4D-CT scans were acquired with a 3 mm slice thickness but for the purpose of this study interpolated to a 1 mm slice thickness to ensure sufficient resolution for distinguishing the different margin strategies. GTVs for the primary tumor (GTV-T) and the lymph nodes (GTV-N) were delineated on the mid-ventilation (mv) phase of the 4D-CT [14] visually guided by the PET scan. Furthermore, GTVs accounting for respiration (iGTV-T and iGTV-N) were delineated in a three-step process: The GTVs were deformably propagated from the mv phase to all phases of the 4D-CT, followed by accumulation, producing iGTV. The iGTVs were finalized by manual correction for deformation errors using visual inspection of all phases as well as a Maximum Intensity Projection scan (MIP) [10]. All delineations and deformations were performed in ARIA 13.7 (Varian Medical Systems) by one experienced radiation oncologist to ensure consistency. For both GTV and iGTV, an isotropic 5 mm expansion, corrected for invasion into bones and large blood vessels, generated the clinical target volumes CTV-T, CTV-N, iCTV-T and iCTV-N. After delineation, all scans and delineations were exported to MIM (MIM Software Inc., Cleveland, OH, USA), where all subsequent margin generation and analysis were performed. CTV-PTV margins were generated separately for CTV-T and CTV-N and combined to a total PTV.

Measuring the respiratory amplitude

GTV-T and GTV-N were propagated deformably to all phases of the 4D-CT scan. The CM position was found on each phase and the respiratory amplitude was found in 6 directions: Left (A_L), Right (A_R), Dorsal (A_D), Ventral (A_V), Superior (A_S) and inferior (A_I).

Investigation of target deformation during respiration

The tumor may deform during the respiratory cycle, (Figure 1). The deformation is included in iGTV. We compared the volumes of iGTV and GTV expanded by A (A_L, A_R, A_D, A_V, A_S, A_I), denoted GTV + resp in order to investigate the effect of deformation. The overlap between iGTV and GTV + resp was obtained and compared to the volume of iGTV and GTV + resp. The analysis was performed for both tumor and lymph nodes in all patients (Figure 1).

Methods to include respiratory motion

Three methods were investigated:

- Delineation on all phases approach: The respiratory motion from all phases was taken into account in the delineation of iGTV. The iGTV was expanded to iCTV and shaped to bones and large vessels.
- Random uncertainty approach: The GTV was expanded to CTV and shaped to bones and large vessels. Respiration was taken into account as a random uncertainty of $A_x/3$ in the CTV-PTV generation as described by [4,14–15].
- Systematic uncertainty approach: The GTV was expanded to CTV and shaped to bones and large vessels. The CTV was subsequently expanded to CTV + resp by adding A_x in all six directions [15].

Planning target volumes

To compare the planning target volumes (PTVs) for the different methods, CTV to PTV margins were calculated for all three methods and used to expand the CTV to PTV. All systematic ($\sum$) and random (σ) uncertainties contributing to the PTV margin are listed in Table 2. The margins calculated are based on daily treatment set-up on the primary tumor as described in [6,16] and different uncertainties are listed for primary tumor and lymph nodes. The margins were calculated using the margin formula of van Herk et al. with a soft tissue penumbra of σ_p=3 mm [5]: $M = 2.5 \sum + 1.64\ (\sigma - \sigma_p)$

Three methods for calculation of PTV was studied (Figure 2)

- Delineation on all phases approach: The respiratory motion was taken into account in the patient specific iCTV-T and iCTV-N. The margin calculated in Table 2 was

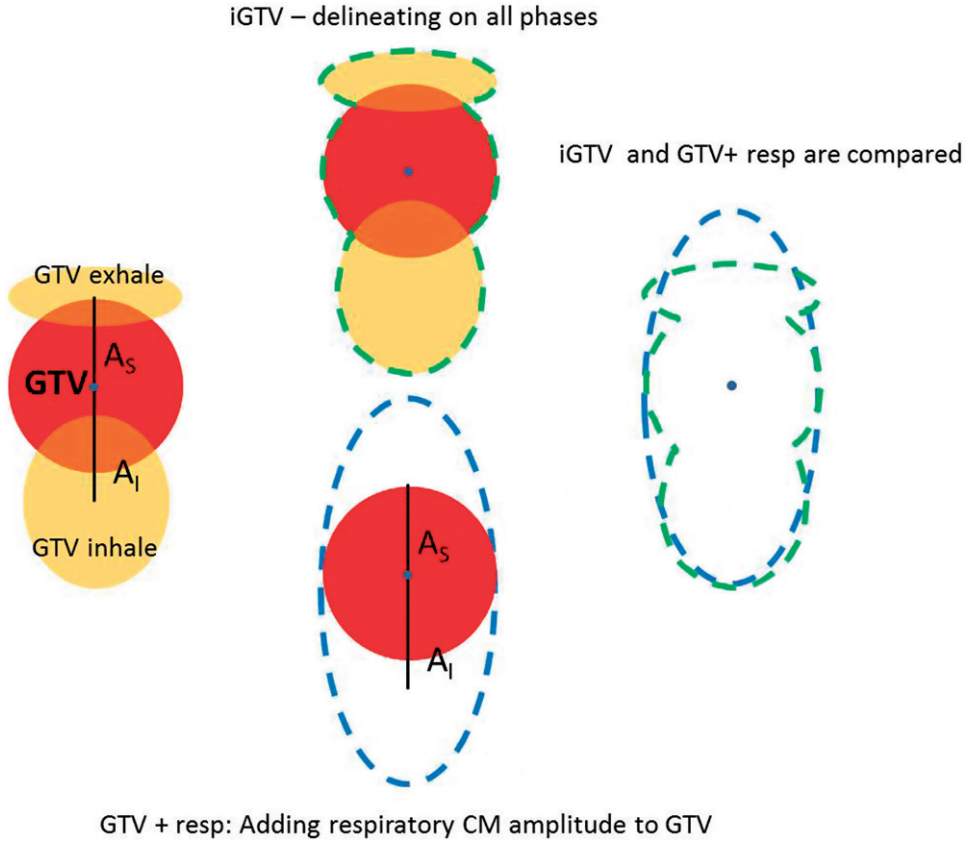

Figure 1. Left: Schematic illustration of deformation of tumor during the respiratory cycle. For simplification only three phases and only S-I motion is shown. All directions of motion were taken into account in the study. Middle: total volume of iGTV and GTV + resp. Right: Overlay of iGTV and GTV + resp, showing regions included in only one of the structures. Centre of mass of the medventilation phase is illustrated by a blue dot.

Table 2. Uncertainties used for margin calculation.

	Tumor (LR, DV,SI)		Lymph nodes (LR, DV,SI)		
	Σ	σ	Σ	σ	Origin
Baseline shift and residual deformation after match	0.8, 0.8, 0.8 mm	1.4, 1.4, 1.4 mm	1.3, 1.0, 1.1 mm	1.3, 1.5, 1.3 mm	* [6]
intrafractional baseline shift	0.5, 0.6, 1.1 mm	1.1, 0.8, 1.2 mm	0.5, 0.6, 1.1 mm	1.1, 0.8, 1.2 mm	*(submitted for publication)
Lymph node surrogate	–	–	0.6, 0.5, 0.7 mm	0.8, 0.8, 0.9 mm	*[6]
CBCT isocentre uncertainty	0.7		0.7		#
Uncertainty in match and couch shift		0.6		0.6	#
CT distortion		0.2		0.2	#
MLC positional uncertainty		0.2		0.2	#
Margin without respiration included.	3.8, 3.8, 4.8 mm		5.2, 4.6, 5.7 mm		

*Data from similar patient group.
#Determined locally, not published.

used to expand the iCTVs and create a total PTV for this method: **PTV_{del}**.

- Random uncertainty approach: Respiration was taken into account as a random uncertainty of $A_x/3$ for each of the six directions. For each of the directions left, right, dorsal, ventral, superior and inferior a patient-specific margin was calculated and used to expand the CTV-T and CTV-N and create a total PTV for this method: **PTV_{σ}**.
- Systematic uncertainty approach: CTV-T + resp and CTV-N + resp were expanded to PTV-T and PTV-N by use of the margins in Table 2 and a total PTV was created: **PTV_{Σ}**.

Results

Eleven patients presented with both GTV-T and GTV-N, while one patient had only GTV-N and three patients had only GTV-T. The mean [min;max] GTV (T + N) volume was 62 cm^3 [4;361 cm^3]. The peak-to-peak respiratory motion for GTV-T was in mean [min;max] 2 mm [1;6 mm] (left-right (LR)), 3 mm [1;6 mm] (anterior-posterior (AP)) and 5 mm [1;16 mm] (superior-inferior (SI)). For GTV-N, the corresponding amplitudes were 2 mm [0;5 mm] (LR), 2 mm [1;5 mm] (AP) and 5 mm [1;9 mm] (SI). The volumes and respiratory motion of GTV-T, GTV-N were displayed for each patient in Table 1.

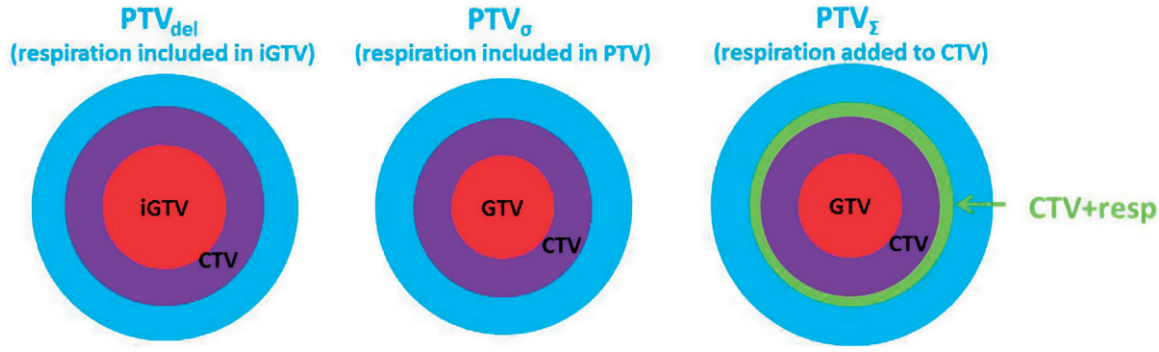

Figure 2. Illustration of three different PTVs generated.

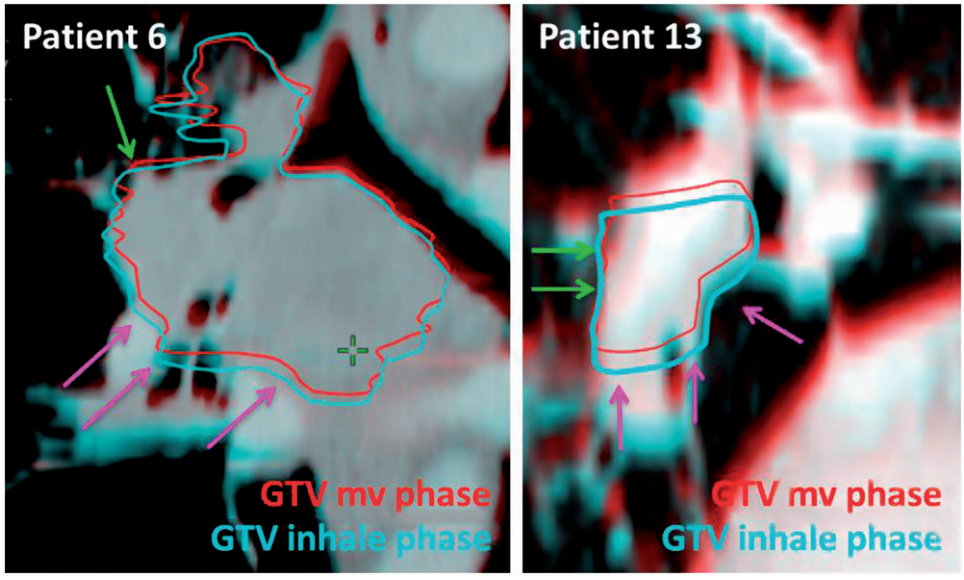

Figure 3. Patient examples illustrating how different parts of the tumor have different respiratory motion patterns leading to tumor deformation between the different respiratory phases. Green arrows indicate areas with small respiratory motion. Pink arrows indicate areas with large respiratory motion.

The delineation of GTV-T and GTV-N on all phases revealed a volumetric change between phases. The GTV-T and GTV-N on the mv phase were on average 17% (*T*) and 9% (*N*) smaller than the phase with largest volume and 14% (*T*) and 15% (*N*) larger than the phase with the smallest volume. These volume changes are due to tumor and lymph nodes deforming during respiration as shown for two patient examples in Figure 3. To investigate this effect further, the overlap of iGTV and GTV + resp were investigated. The percentage of the iGTV (inclusion of full respiratory cycle) included in the GTV + resp (inclusion of respiration only by the CM amplitudes) was in mean [min;max] 93% [89;99%] for *T* and 93% [89;98%] for *N*. This illustrates that on average 7% of the iGTV is outside of GTV + resp and thus, GTV + resp did not fully represent the tumor during the respiratory motion. The percentage of the GTV + resp not included in the iGTV was 89% [76;94%] for *T* and 82% [57;91%] for *N*. This shows that the GTV + resp included tissue that was not part of the actual respiratory tumor motion. Taking the respiration into account as a random uncertainty in the PTV calculation, makes the effect of this overestimation on the treatment volume negligible. This is due to a low weight of the random component and many factors adding up in the margin calculation.

The comparison of the three PTV volumes is shown in the box plot in Figure 4. For all patients, **PTV$_{\sigma}$** was smallest and **PTV$_{\Sigma}$** largest. The difference between PTV$_{\sigma}$ and PTV$_{del}$ was statistical significant when compared with a Wilcoxon signed rank test ($p<.001$). Likewise, for PTV$_{del}$, PTV$_{\Sigma}$ ($p<.001$). On average, the **PTV$_{\sigma}$** was 14% (31 cm^3) smaller than **PTV$_{del}$**, while **PTV$_{del}$** was 7% (20 cm^3) smaller than **PTV$_{\Sigma}$**.

Discussion

Delineating the tumor during the entire respiratory motion on the 4D-CT scan ensures treatment of the tumor throughout the full respiratory cycle. However, it also results in treatment of the whole respiratory cycle as a systematic uncertainty. This yields PTVs (PTV$_{del}$) that are on average 14% larger than PTVs achieved by including the respiration amplitude as a random uncertainty in the margin calculation (PTV$_{\sigma}$). The PTVs are further enlarged (7% on average) if the systematic inclusion of the respiratory motion is based on the measured amplitudes (PTV$_{\Sigma}$), rather than delineating the actual motion (PTV$_{del}$). Wolthaus et al. found that PTV$_{\Sigma}$ yielded volumes that were on average 33% larger than PTV$_{\sigma}$ [15], which is much larger than the 18% we found in

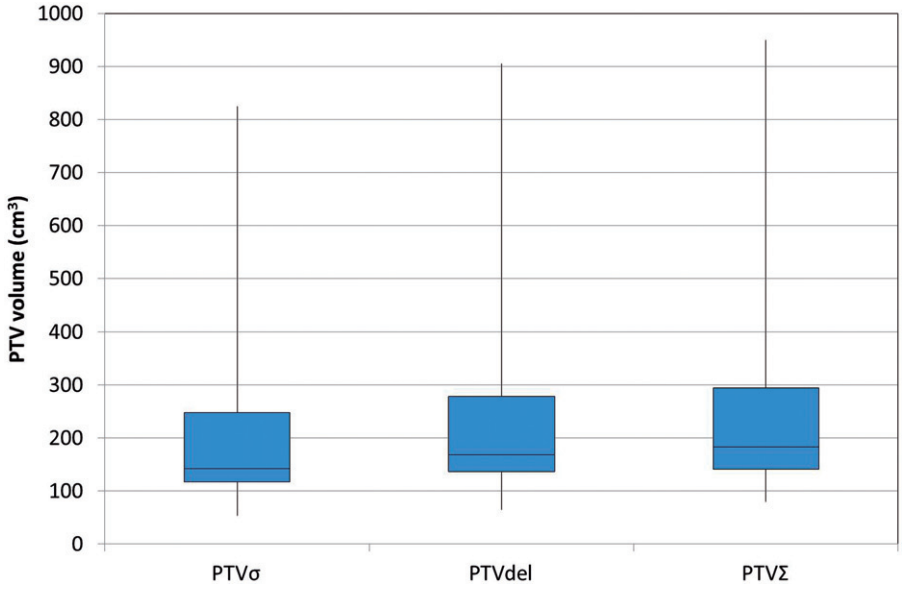

Figure 4. Comparison of PTV volumes. Box plot: median (horizontal line), 1st and 3rd interquartile ranges (blue box) and min/max (vertical line).

this study. This discrepancy could be due to smaller GTV volumes and larger superior-inferior tumor motion in [15]. In clinical practice, PTV_{σ} and PTV_{del} are commonly used [11–13]. PTV_{Σ} has been used as a surrogate for PTV_{del} [15] but as shown here, PTV_{Σ} overestimates the PTV_{del} volume size.

Several studies show correlation between the PTV volume treated and the incidence of radiation pneumonitis [17–19]. Tvilum et al showed in a nonrandomized study introducing soft-tissue match and adaptive radiotherapy that reducing the PTV volumes by on average 199 cm^3 (599–400 cm^3) led to a decrease in mean lung dose (14.4 Gy to 12.6 Gy) and a 4% (22–18%) reduction in severe pneumonitis [17]. The clinical effect of a 14% PTV reduction therefore appears to be minor except in the case of large tumor burdens. Less than one out of four patients had PTV larger than 300 cm^3, for which a 14% reduction corresponds to 42 cm^3. The same study also illustrated that the PTV volume reduction due to a change of setup strategy from bone match to soft-tissue match, had a much higher volumetric impact (199 cm^3 on average) compared to choosing PTV_{σ} instead of PTV_{del} (31 cm^3 on average). The same can be concluded for the dosimetric deterioration during treatment due to target and normal tissue position uncertainties: respiratory uncertainties have been shown to exhibit negligible impact compared to inter-fractional baseline shifts and especially anatomical changes [20]. The dose deterioration due to respiration was investigated for SBRT, where recalculation of dose plans optimized on a 3D CT scan and subsequently recalculated on a full 4D-CT. The 4D-CT recalculation maintained the target dose coverage [21].

PTV_{σ} and PTV_{Σ} are based on reducing the respiratory motion to a rigid movement of the tumor on the mv phase with the amplitude measured on the 4D-CT. As shown in this study, there is a high degree of tumor deformation during the respiration and the volume changes between the phases. On average, 7% of the tumor delineated on all phases is not accounted for using the measured amplitudes only. In many cases, the deformation originates from part of the tumor (e.g. the caudal part) moving more than other parts (e.g. the cranial part) as shown in Figure 3. The same observation was made by Donnely et al, who described a larger motion of the edge of both primary tumor and lymph node targets compared to the CM motion [22]. Volumetric differences between tumor volume in different respiratory phases were also observed by Reitzel et al. [23].

All methods described for respiratory motion inclusion is based on a single 4D-CT scan before treatment. This assumption is based on several studies showing good inter-fractional stability of the respiratory amplitude with only small variations in the respiratory amplitude [9,24–26]. The respiratory amplitude has been measured separately for tumor and lymph nodes because the respiratory motion of the two typically deviates from each other [7,22].

In conclusion, incorporating respiratory motion in the target delineation process ensures that the entire respiratory motion, including tumor deformation, is accounted for, at the cost of larger PTV volumes. The PTV_{σ} yields the smallest volumes, but does not take the full respiratory motion and tumor deformation into account. PTV_{Σ} should not be used, since it incorporates the disadvantages of both PTV_{del} and PTV_{σ}.

Disclosure statement

No potential conflict of interest was reported by the authors.

Funding

This work was supported by The Danish Cancer Society [grant number R124 A7821].

ORCID

Marianne Marquard Knap http://orcid.org/0000-0001-6215-8071
Lone Hoffmann http://orcid.org/0000-0002-3575-0421

References

[1] Bradley JD, Paulus R, Komaki R, et al. Standard-dose versus high-dose conformal radiotherapy with concurrent and consolidation carboplatin plus paclitaxel with or without cetuximab for patients with stage IIIA or IIIB non-small-cell lung cancer (RTOG 0617): a randomised, two-by-two factorial phase 3 study. Lancet Oncol. 2015;16:187–199.

[2] Khalil AA, Hoffmann L, Møller DS, et al. New dose constraint reduces radiation-induced fatal pneumonitis in locally advanced non-small cell lung cancer patients treated with intensity-modulated Radiotherapy. Acta Oncol. 2015;54:1343–1349.

[3] Marks LB, Bentzen SM, Deasy JO, et al. Radiation dose-volume effects in the lung. Int J Radiat Oncol Biol Phys. 2010; 76:S70–S76.

[4] van Herk M. Errors and margins in radiotherapy. Semin Radiat Oncol. 2004;14:52–64.

[5] van Herk M, Remeijer P, Rasch C, et al. The probability of correct target dosage: dose-population histograms for deriving treatment margins in radiotherapy. Int J Radiat Oncol Biol Phys. 2000;47: 1121–1135.

[6] Hoffmann L, Holt MI, Knap MM, et al. Anatomical landmarks accurately determine interfractional lymph node shifts during radiotherapy of lung cancer patients. Radiother Oncol. 2015;116: 64–69.

[7] Schaake EE, Rossi MMG, Buikhuisen WA, et al. Differential motion between mediastinal lymph nodes and primary tumor in radically irradiated lung cancer patients. Int J Radiat Oncol Biol Phys. 2014; 90:959–966.

[8] Seppenwoolde Y, Shirato H, Kitamura K, et al. Precise and real-time measurement of 3D tumor motion in lung due to breathing and heartbeat, measured during radiotherapy. Int J Radiat Oncol Biol Phys. 2002;53:822–834.

[9] Sonke JJ, Lebesque J, van Herk M. Variability of four-dimensional computed tomography patient models. Int J Radiat Oncol Biol Phys. 2008;70:590–598.

[10] Underberg RW, Lagerwaard FJ, Slotman BJ, et al. Use of maximum intensity projections (MIP) for target volume generation in 4DCT scans for lung cancer. Int J Radiat Oncol Biol Phys. 2005;63: 253–260.

[11] Ezhil M, Vedam S, Balter P, et al. Determination of patient-specific internal gross tumor volumes for lung cancer using four-dimensional computed tomography. Radiat Oncol. 2009;4:4.

[12] Verstegen NE, Lagerwaard FJ, Hashemi SM, et al. Patterns of disease recurrence after SABR for early stage non-small-cell lung cancer: optimizing follow-up schedules for salvage therapy. J Thorac Oncol. 2015;10:1195–1200.

[13] Peulen H, Belderbos J, Rossi M, et al. Mid-ventilation based PTV margins in stereotactic body radiotherapy (SBRT): a clinical evaluation. Radiother Oncol. 2014;110:511–516.

[14] Wolthaus JW, Schneider C, Sonke JJ, et al. Mid-ventilation CT scan construction from four-dimensional respiration-correlated CT scans for radiotherapy planning of lung cancer patients. Int J Radiat Oncol Biol Phys. 2006;65:1560–1571.

[15] Wolthaus JW, Sonke JJ, van Herk M, et al. Comparison of different strategies to use four-dimensional computed tomography in treatment planning for lung cancer patients. Int J Radiat Oncol Biol Phys. 2008;70:1229–1238.

[16] Møller DS, Holt MI, Alber M, et al. Adaptive radiotherapy for advanced lung cancer ensures target coverage and decreases lung dose. Radiother Oncol. 2016;121:32–38.

[17] Tvilum M, Khalil AA, Møller DS, et al. Clinical outcome of image-guided adaptive radiotherapy in the treatment of lung cancer patients. Acta Oncol. 2015;54:1430–1437.

[18] Dang J, Li G, Zang S, et al. Risk and predictors for early radiation pneumonitis in patients with stage III non-small cell lung cancer treated with concurrent or sequential chemoradiotherapy. Radiat Oncol. 2014; 9:172.

[19] Sunyach MP, Falchero L, Pommier P, et al. Prospective evaluation of early lung toxicity following three-dimensional conformal radiation therapy in non-small-cell lung cancer: preliminary results. Int J Radiat Oncol Biol Phys. 2000;48:459–463.

[20] Schmidt ML, Hoffmann L, Kandi M, et al. Dosimetric impact of respiratory motion, interfraction baseline shifts, and anatomical changes in radiotherapy of non-small cell lung cancer. Acta Oncol. 2013;52:1490–1496.

[21] Guckenberger M, Wilbert J, Krieger T, et al. Four-dimensional treatment planning for stereotactic body radiotherapy. Int J Radiat Oncol Biol Phys. 2007;69:276–285.

[22] Donnelly ED, Parikh PJ, Lu W, et al. Assessment of intrafraction mediastinal and hilar lymph node movement and comparison to lung tumor motion using four-dimensional CT. Int J Radiat Oncol Biol Phys. 2007;69:580–588.

[23] Rietzel E, Chen GT, Choi NC, et al. Four-dimensional image-based treatment planning: Target volume segmentation and dose calculation in the presence of respiratory motion. Int J Radiat Oncol Biol Phys. 2005;61:1535–1550.

[24] Guckenberger M, Wilbert J, Mayer J, et al. Is a single respiratory correlated 4D-CT study sufficient for evaluation of breathing motion?. Int J Radiat Oncol Biol Phys. 2007;67:1352–1359.

[25] van der Geld YG, Lagerwald FJ, van Sörensen, et al. Reproducibility of target volumes generated using uncoached 4-dimensional CT scans for peripheral lung cancer. Radiat Oncol. 2006;1:43.

[26] Schmidt ML, Hoffmann L, Knap MM, et al. Cardiac and respiration induced motion of mediastinal lymph nodet targets in lung cancer patients throughout the radiotherapy treatment course. Radioth Oncol. 2016;121:52–58.

[27] Mountain CF, Dresler CM. Regional lymph node classification for lung cancer staging. Chest. 1997;111:1718–1723.